

What we *do* and *do not* know about the *s*-process in AGB stars

J. C. Lattanzio^a and M. A. Lugaro^b

^aCentre for Stellar and Planetary Astrophysics, Monash University, Australia; and IGPP, Lawrence Livermore National Laboratory, California, USA

^bInstitute of Astronomy, Cambridge University, UK

AGB stars are the source for the main component of the *s*-process. Here we discuss both the properties which are reasonably well known and those which still suffer from substantial uncertainties. In the former case, we are fairly sure that the *s*-process contribution from AGB stars comes from masses between about 1 and 3 M_{\odot} , and the dominant neutron source is the $^{13}\text{C}(\alpha, n)^{16}\text{O}$ reaction. In the latter category remains the formation mechanism for the ^{13}C -pocket. Attempts at including rotation seem to inhibit neutron capture reactions. Explaining the observations seems to require a spread in the size of the ^{13}C -pocket so some stochastic process, such as rotation, must be involved.

1. Introduction to the *s*-process

The *s*-process refers to neutron captures being slow compared to subsequent beta decays, typically with $n_n \lesssim 10^8 \text{ cm}^{-3}$. In this approximation, and assuming no branchings, the equation governing the abundance N_A of the (stable) isobar of mass A is

$$\frac{dN_A}{dt} = -n_n \langle \sigma v \rangle_A N_A + n_n \langle \sigma v \rangle_{A-1} N_{A-1} \quad (1)$$

where n_n is the neutron number density and $\langle \sigma v \rangle_A$ is the thermally averaged neutron-capture cross-section for the isobar of mass A . It is common to write $\langle \sigma v \rangle_A$ as $\sigma_A v_T$ where v_T is the thermal velocity of the neutrons and σ_A is an appropriate average cross-section. It is useful to define the neutron exposure by $\tau = \int n_n v_T dt$, and thus we get

$$\frac{dN_A}{d\tau} = -\sigma_A N_A + \sigma_{A-1} N_{A-1}. \quad (2)$$

In a steady-state $dN_A/dt = 0$ and $\sigma_A N_A$ is constant. The solar system distribution does show $\sigma_A N_A$ roughly constant when away from the isobars of magic neutron number (these produce bottle-necks in the distribution due to their low cross-section).

Clayton et al. [1] showed that a single neutron exposure τ could not reproduce the solar system distribution, and we historically recognise three distinct components:

- 1) *Weak Component*: producing most of the *s*-isotopes with $A \lesssim 90$, from Fe to Sr;
- 2) *Main Component*: responsible for the *s*-isotopes from $90 \lesssim A \lesssim 204$, from Sr to Pb;
- 3) *Strong Component*: devised primarily to produce ^{208}Pb in the solar system.

To reproduce the solar system distribution we add a mix of these three components. The weak component is believed to come from central He burning in massive stars, where the neutron source is $^{22}\text{Ne}(\alpha, n)^{25}\text{Mg}$. The main component is associated with AGB stars, and the strong component is now associated with metal-poor AGB stars.

2. The ^{22}Ne neutron Source

There is strong evidence that most giant stars enriched in s -process elements have masses around $1 - 3 M_{\odot}$. In these stars the neutron source is $^{13}\text{C}(\alpha, n)^{16}\text{O}$, as discussed in the next section. But for intermediate-mass AGB stars ($M \gtrsim 3 M_{\odot}$) the neutron source is thought to be ^{22}Ne .

In many ways, the ^{22}Ne source is the simplest to activate. The H-shell burns CNO into ^{14}N which can then capture two alpha-particles during the next thermal pulse to produce ^{22}Ne in the flash-driven convective pocket. If the peak temperature in this pocket exceeds 300 million K then neutrons are released by $^{22}\text{Ne}(\alpha, n)^{25}\text{Mg}$. However, a few things work against the ^{22}Ne source being important for the s -process. Firstly there is the fact that the extent in mass of the flash-driven convective zone decreases as the stellar mass increases, from about $0.03 M_{\odot}$ (in low mass stars) to below $0.005 M_{\odot}$ for intermediate masses. Thus, the number of seeds and neutrons is small, so that not much processing can occur. Secondly, to make the situation worse, the duration in time of the pocket also decreases with mass, from about 300y to 20y, giving less time for the neutrons to be produced. This is at least partly offset by the fact that the temperature of the shell increases with mass, making more neutrons available at higher masses. Thirdly, the small convective zone of enriched s -process elements is then diluted in a large envelope prior to its ejection into the interstellar medium via the stellar wind. And finally, the shape of the IMF also works against intermediate mass stars being an important site for the s -process. Nevertheless, a quantitative estimate of their importance is not available at present, and would be useful. Further, it is possible that the ^{13}C source could be active in these stars in addition to the ^{22}Ne source. It would also suffer from the extreme closeness of the H and He shells in intermediate-mass stars, and hence, is unlikely to be important. But a quantitative analysis is not yet available.

3. The ^{13}C neutron Source

3.1. Basics of the ^{13}C Source

The basic mechanism of the ^{13}C source is fairly simple, and is shown in Figure 1. Some protons are mixed below the hydrogen-rich envelope at the time that dredge-up ceases. This region is comprised of about 25% ^{12}C and 75% ^4He (by mass). The protons are captured by the abundant ^{12}C nuclei to form ^{13}C and ^{14}N . When the star contracts again, the H shell reignites and the temperature in the ^{13}C pocket approaches 100 million K where the timescale for α -capture decreases below the time between pulses [2]. Hence, neutrons are released within the pocket at quite low neutron densities. These neutrons are captured *in situ* by Fe and heavy species to produce the s -process isotopes. At the next pulse this s -process rich shell is ingested by the convective pocket. In addition, even in low mass stars there might be a brief activation of the ^{22}Ne source at the peak of the pulse. This much is relatively clear. The details, however, are another matter.

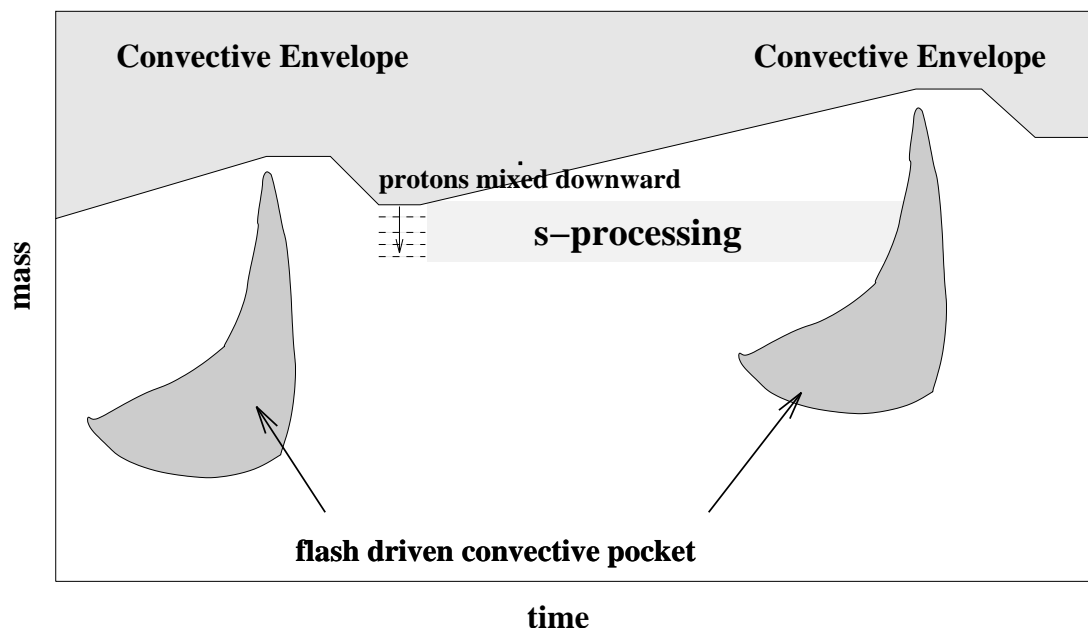


Figure 1. Schematic diagram showing the operation of the ^{13}C neutron source.

3.2. Formation of the ^{13}C Pocket

The largest unknown in the scenario described above is the mechanism which causes the protons to be mixed into the carbon-enriched region. We will discuss four mechanisms which have been suggested and explored.

3.2.1. Semiconvection

The first calculation which showed the activation of the ^{13}C source was [3],[4]. They found that, following a pulse, the expansion of the star caused some recombination of fully ionized carbon atoms at the very bottom of the hydrogen-rich envelope. This caused a dramatic change in the opacity, and a small semiconvective region developed at the bottom of the formally convective envelope. This mixed some protons down and produced a thin region, a few $\times 10^{-4} M_{\odot}$, containing a mass fraction of a few $\times 10^{-3}$ in ^{13}C . There is also a small ^{14}N pocket just atop the ^{13}C pocket; this region plays little role in the subsequent s-processing (^{14}N is a neutron poison).

This mechanism was not found to occur very often in detailed model calculations. Nevertheless, the fact that simple 1D convective models often show convergence problems at the bottom of the convective zone during dredge-up ([5]) is, we believe, an indication that the models are inadequate in this region. Semiconvection may yet be the main mechanism for activating the ^{13}C source.

3.2.2. Convective Overshoot

An obvious possible mechanism for mixing beyond a formal convective boundary is overshooting. Note that “overshooting” usually refers to mixing beyond a supposed convective-radiative boundary, which is usually determined by the Schwarzschild or Ledoux

criterion. In this case we do not mean homogeneous mixing, or a simple extension of the convective zone into the radiative zone. Rather, for the ^{13}C source to be activated we must mix a relatively small number of protons into the Carbon-enriched zone.

Stimulated by the 2D hydrodynamic convective models of [6] which showed such partially mixed zones, [7] introduced an exponential decay in the convective velocity. This produces the partial mixing required by the ^{13}C source. It also, unfortunately, introduces parameters associated with the overshooting which determine the size of the ^{13}C pocket.

3.2.3. Gravity Waves

A recent suggestion by [8] is that gravity waves at the bottom of the convective envelope can produce partial mixing beyond the convective boundary. For reasonable assumptions the resultant ^{13}C pocket is about the size required to match observed abundances.

3.2.4. Rotation

In stellar models computed with rotation, during the AGB phase a large angular velocity gradient forms, just after the occurrence of the third dredge-up, at the interface between the faster-rotating core and the slower-rotating envelope. A zone where partial mixing of protons and ^{12}C is thus generated at the core/envelope interface because of shear mixing. As with the other types of mechanism for the production of the ^{13}C pocket, the proton profile is continuous in the region so that a ^{13}C pocket is created where the ratio of the number of protons to ^{12}C is below unity, and an adjacent ^{14}N pocket is created where the ratio of protons to ^{12}C is above unity. However, while with the other types of mechanism these two pockets keep separated during the neutron release by $^{13}\text{C}(\alpha, n)^{16}\text{O}$ in the interpulse period, in the rotating models shear mixing persists throughout the interpulse period because the steep angular velocity gradient remains at the mass coordinate of the pocket formation. Consequently, a large amount of ^{14}N is mixed down into the ^{13}C -rich region [9, 10]. These ^{14}N nuclei act as a strong neutron poison during the s -process because of the relatively high cross section of the $^{14}\text{N}(n, p)^{14}\text{C}$ reaction. The last measurement of this reaction gave 2.04 ± 0.16 mbarn at 24.5 keV [11] confirming previous calculations [12] and measurements [13]. In conclusion, the s -process is completely inhibited in models that include rotation [9]. This result has been produced for a model of $3 M_{\odot}$ with initial surface rotation velocity of 250 km s^{-1} , but also confirmed for lower initial velocities.

Since all stars rotate, this is a major problem for the current models! One should also consider though that magnetic fields are generated by rotation, but have not been included in the computations of AGB stars so far and could represent a way to “save the s -process”. Magnetic fields, in fact, could enhance the coupling of core and envelope thus decelerating the core and reducing the strength of the rotational shear mixing [14]. The problem is open and requires further exploration.

If the effect of rotation could be reduced, then a spread of neutron exposures could be produced by different amount of ^{14}N mixed into the ^{13}C pocket as a result of a spread of rotational mixing coefficients [9]. Then, different neutron exposures result in different final s -process abundance distributions [10]. As we describe below in more detail, several types of observational constraints seem to require such a spread of efficiencies to occur:

1. the spectroscopic observations of the s -element distributions in AGB and post-AGB

stars of different metallicities,

2. the spectroscopic observations of lead in stars of low metallicity,
3. the isotopic composition of single presolar silicon carbide grains from carbon stars.

In summary, a possible scenario within the current models is that the spread of efficiencies in the ^{13}C neutron source required by the observations is somewhat related to the effect of rotation and magnetic fields in stars, even through more defined conclusions will be set only via much future detailed work.

4. AGB Star *s*-Process Results

The latest generation of *s*-process models are based on AGB stellar structure computed by evolutionary codes with the artificial introduction of a parametrized ^{13}C pocket [15, 16]. The two phases of neutron-capture processes experienced by the intershell material during an interpulse-pulse period can be summarised as following.

The ^{13}C source. After less than a few thousand years from the occurrence of proton diffusion into the intershell at the end of dredge-up, the ^{13}C pocket is formed. The $^{13}\text{C}(\alpha, n)^{16}\text{O}$ reaction is activated during the interpulse phase in radiative conditions at low temperature, $\sim 9 \times 10^7$ K, and all the ^{13}C is typically consumed before the end of the interpulse period [2]. This is the main site for the *s*-process. The neutron flux lasts typically 10,000 yr and can produce very high neutron exposures, up to $\sim 0.5 \text{ mb}^{-1}$ in solar-metallicity stars, but with low neutron density values, only up to about 10^7 n/cm^3 (in solar-metallicity stars).

The ^{22}Ne source. At the end of the interpulse the ^{13}C pocket is engulfed by the following convective pulse and thus mixed with intershell material from the previous convective pulse and the ashes from the H-burning shell. In the convective pulse, the $^{22}\text{Ne}(\alpha, n)^{25}\text{Mg}$ reaction is marginally activated at temperatures $\geq 2.5 \times 10^8$ K, and a second neutron flux occurs, whose strength depends on the temperature at the base of the convective pulse. A large amount of ^{22}Ne is present in the convective pulse as a product of double α -captures starting on the abundant ^{14}N from the H-burning ashes. This second neutron burst is opposite in features to that in the ^{13}C pocket: it occurs on a timescale of a few years and it produces typically very low neutron exposures, of the order of 10^{-2} mb^{-1} in solar metallicity stars, with a high-peaked neutron density, up to 10^{11} n/cm^3 , in solar-metallicity stars. This neutron burst does not contribute much to the overall production of *s* elements, however it has a large effect on the final abundances of isotopes connected to branching points.

After each thermal pulse the *s*-process rich material from the He intershell is dredged up to the envelope by the next dredge-up event. This cycle is repeated over all thermal pulses with dredge-up and the heavy element composition of the envelope throughout the AGB phase is changed.

4.1. Variations with the metallicity

As first observed by [17]: “Take the stellar structure to be independent of Z , as is the intershell ^{12}C content because it is manufactured by the burning within the star. Thus the neutron source is in this case independent of the initial metallicity, but the major absorbers ($^{22}\text{Ne} + \text{Fe}$) are metallicity dependent [...] the neutron density is proportional to Z^{-1} . That is, *more metal-poor stars produce larger neutron fluences!*” Current models with primary ^{13}C as the main source do indeed produce heavier and heavier elements at lower and lower Z , until mostly Pb is produced. This result is independent of the uncertainties associated with the formation of the ^{13}C pocket, if we assume that the mechanism that generates the proton diffusion in the intershell always produces a primary ^{13}C neutron source in stars of different metallicities. This assumption could appear rather bold, given the poor knowledge of this mechanism. However, current models including this assumption seem to work quite well in explaining major observational features. Hence, it may actually turn out that this assumption *should* be verified by models for the formation of the ^{13}C source.

Working within this hypothesis, the following results are obtained when we keep fixed the amount of the ^{13}C neutron source while changing the initial metallicity of the star. At metallicities close to solar, Sr-peak elements are produced. At metallicities about 1/4 of solar Ba-peak elements are produced, while at lower metallicities Pb is produced (see Figures 1 and 2 of [18]).

4.2. Stellar observations at different metallicity

The current model predictions well match the general features of the observed distribution of heavy elements in AGB stars of different metallicities. However, a spread in the efficiency of the neutron flux in the ^{13}C pocket has to be introduced at each metallicity to cover the spread in the distribution shown by the observational data [18]. This spread of efficiencies in the neutron flux produced in the ^{13}C pocket is represented by choices of the ^{13}C efficiencies ranging from the maximum neutron exposure allowed by the presence of the ^{14}N poison to lower values down to zero. For example, at solar metallicity $\tau \leq 0.5 \text{ mb}^{-1}$. As discussed above, this spread toward neutron exposures lower than predicted can be produced by different efficiency in the mixing of ^{14}N produced in the upper region of the partial mixing zone down to the ^{13}C -rich region.

The Pb overabundances recently observed in stars of low metallicity represent another important indication that the ^{13}C neutron source is in fact of primary nature, as the production of Pb in these stars was predicted by the current models [15]. The distribution of the Pb overabundances and the ratio Pb/Ce show a spread of efficiencies at any given metallicity [19] requiring again a spread of efficiency of the ^{13}C neutron source at any metallicity.

4.3. The Galactic Chemical Evolution of heavy elements

The consequences of applying the recent s -process models to the chemical evolution of heavy elements in the Galaxy have been presented in a series of paper by Travaglio, and collaborators. The main conclusions are:

- The Galactic abundance of Ba-peak elements is explained by s - and r -processes with a contribution of 80% to solar Ba from the s -process in AGB stars of metallicity $\sim 1/4$ of solar [20].

- The Galactic abundance of Pb is explained by *s*- and *r*-processes with a contribution of 90% to the solar abundance of Pb from the *s*-process in AGB stars of metallicity $\sim 1/10$ of solar [21]. The classical *strong component* is now incorporated in the framework of the *s*-process in AGB stars.
- Elements belonging to the Sr peak instead appear **not** to be explained by the *s*- and *r*-processes! A special primary component from massive stars is needed to match observations of the light *s*-process elements at low metallicity. About 70% of solar Sr comes from the *s*-process in AGB stars of metallicity $\sim 1/2$ solar [22].

5. Presolar SiC Grains from AGB stars

New constraints on the *s*-process in AGB stars come from meteoritic silicon carbide (SiC) grains that formed in the expanding envelopes of carbon stars and contain trace amounts of heavy elements showing the signature of the *s*-process. High-sensitivity laboratory measurements of the isotopic composition of trace heavy elements in single SiC of the size of micrometers provide constraints of precision never achieved before on models of the *s*-process and on neutron-capture cross sections.

For example, the $^{96}\text{Zr}/^{94}\text{Zr}$ ratio is very sensitive to the nucleosynthesis in the convective pulse, which in turn depends on the still uncertain $^{22}\text{Ne}(\alpha, n)^{25}\text{Mg}$ reaction rate and the temperature at the base of the convective instability. This is because ^{96}Zr is produced through a branching at ^{95}Zr during the neutron flux of high peak neutron density released by the $^{22}\text{Ne}(\alpha, n)^{25}\text{Mg}$ reaction, while ^{94}Zr is produced during the main neutron flux released by the $^{13}\text{C}(\alpha, n)^{16}\text{O}$ reaction. Data from single SiC grains always show deficits in the $^{96}\text{Zr}/^{94}\text{Zr}$ ratio with respect to solar and point to a marginal activation of the ^{22}Ne neutron source [23], thus excluding intermediate-mass AGB stars as the parent stars of the grains, as well as the NACRE upper limit of the $^{22}\text{Ne}(\alpha, n)^{25}\text{Mg}$ reaction as the correct value for this reaction. Four presolar SiC grains show extreme deficits in the $^{96}\text{Zr}/^{94}\text{Zr}$ ratios and are still unmatched by any of the current models.

The $^{90,91,92}\text{Zr}/^{94}\text{Zr}$ ratios on the other hand involve nuclei near closed neutron shells and thus depend on the main neutron exposure released by the ^{13}C neutron source. The observed values for these ratios in single SiC grains are recovered by considering (again!) a spread of efficiencies in the neutron flux produced by the ^{13}C source.

The precision with which presolar grain data are obtained also stimulates new measurements of neutron-capture cross sections (Koehler, P., these proceedings). The laboratory techniques for the analysis of presolar grains are expanding rapidly, especially with the recent introduction of new instruments for material analysis targeted at the study of presolar grains: the NanoSIMS, a secondary ionization mass spectrometer with a primary ion beam of the size of nanometers [24] and the RIMS technique, resonant ionization mass spectrometry combined to a laser-extraction technique [25]. The current and future opportunities of constraining *s*-process models using laboratory data from the analysis of presolar grains are vast and compelling.

6. Conclusions

Some details of the *s*-process in AGB stars seem now to be well understood, and yet others remain a mystery. It is rather unsatisfactory that we still do not know the mechanism(s) responsible for the production of the ^{13}C pocket. As a consequence we do not know how this might vary with stellar parameters, although there are clearly indications from observations that there are variations from star to star. Nevertheless, with simultaneous attacks on the problem coming from spectroscopy, grain analysis and advanced computer modelling, we may be optimistic that we will yet overcome our current limitations.

This work was supported by the Australian Research Council, and was performed under the auspices of the U.S. Department of Energy, National Nuclear Security Administration by the University of California, Lawrence Livermore National Laboratory under contract No. W-7405-Eng-48.

REFERENCES

1. Clayton D.D., Fowler W.A., Hull T.E., Zimmerman B.A., 1961, *Ann Phys* 12, 331
2. Straniero, O., Gallino, R., Busso, M., Chieffi, A., Raiteri, C. M., Salaris, M., & Limongi, M., *ApJ* 440 (1995) L85
3. Iben, I., Jr., & Renzini, A., *ApJ* 259 (1982) L791
4. Iben, I., Jr., & Renzini, A., *ApJ* 263 (1982) L231
5. Frost, C. A., & Lattanzio, J. C., *ApJ* 473 (1996) 383
6. Freytag, B., Ludwig, H.-G., & Steffen, M., *A&A*, 313 (1996) 497
7. Herwig, F., Blöcker, T., Schönberner, D., & El Eid, M., *A&A* 324 (1997) L81
8. Denissenkov, D. & Tout, C. A., *MNRAS* 340 (2003) 722
9. Herwig, F., Langer, N. & Lugaro, M., *ApJ* 593 (2003) 1056.
10. Siess, L., Goriely, S., & Langer, N., *A&A* 415 (2004) 1089.
11. Gledenov, Y., Salatski, V., Sedyshev, P., Sedysheva, M., Koehler, P., Vesna, V., & Okunev, I., in *AIP Conf. Proc.* 327, *Nuclei in the Cosmos III*, ed. M. Busso, R. Gallino, & C. M. Raiteri (1995) (Woodbury: AIP), 173
12. Bahcall, N. A., & Fowler, W. A., *ApJ* 157 (1969) 659.
13. Koehler, P. E., & O'brien, H. A., *Physical Review C* 39 (1989) 1655.
14. Spruit, H. C., *A&A* 333 (1998) 603.
15. Gallino, R., Arlandini, C., Busso, M., Lugaro, M., Travaglio, C., Straniero, O., Chieffi, A., & Limongi, M. *ApJ* 497 (1998) 388.
16. Goriely, S., & Mowlavi, N., *A&A* 362 (2000) 599.
17. Clayton, D., *MNRAS* 234 (1998) 1.
18. Busso, M., Gallino, R., Lambert, D. L., Travaglio, C., & Smith, V. V., *ApJ* 557 (2001) 802.
19. Van Eck, S., Goriely, S., Jorissen, A., & Plez, B., *A&A* 404 (2003) 291.
20. Travaglio, C., Galli, D., Gallino, R., Busso, M., Ferrini, F., Straniero, O., *ApJ* 521 (1999) 691.
21. Travaglio, C., Gallino, R., Busso, M. & Gratton, R., *ApJ* 549 (2001) 346.
22. Travaglio, C., Gallino, R., Arnone, E., Cowan, J., Jordan, F., & Sneden, C., *ApJ* 601

- (2004) 864.
23. Lugaro et al. *ApJ* 593 (2003) 486.
 24. Hoppe, P., *New Astronomy Reviews* 46 (2002) 589.
 25. Savina, M. R.; Pellin, M. J.; Tripa, C. E.; Veryovkin, I. V.; Calaway, W. F.; Davis, A. M. *Geochimica et Cosmochimica Acta*, 67 (2004) 3215.